Supplement of Atmos. Chem. Phys., 26, 5531–5551, 2026
https://doi.org/10.5194/acp-26-5531-2026-supplement

Atmospheric Chemistry and Physics
Open Access
EGU

Supplement of

Global CO emissions and drivers of atmospheric CO trends constrained by MOPITT satellite measurements

Zhaojun Tang et al.

Correspondence to: Zhe Jiang (zhejiang@tju.edu.cn)

Supplemental Information

	MOPITT Column + fixed OH (Tg/yr)						MOPITT Profile + fixed OH (Tg/yr)						MOPITT Column + Variable OH (Tg/yr)					
Years	US	Europe	E. China	India	SE. Asia	Global	US	Europe	E. China	India	SE. Asia	Global	US	Europe	E. China	India	SE. Asia	Global
2003	88.1	51.3	215.9	65.4	25.8	654.1	79.7	47.4	205.3	64.1	25.5	612.2	82.6	50.4	203.2	61.1	25.3	627.5
2004	81.5	49.5	221.0	64.6	26.5	652.5	76.0	46.0	212.9	64.7	26.1	617.3	77.3	48.7	211.0	59.9	26.1	630.3
2005	77.7	46.7	219.3	66.8	26.0	640.7	73.5	43.6	212.5	65.7	26.1	611.3	73.3	45.9	209.8	62.5	25.6	618.6
2006	78.5	45.0	218.4	63.7	25.9	640.9	72.8	42.1	212.4	64.8	26.1	609.0	73.7	44.4	208.6	58.1	25.3	616.2
2007	75.8	44.3	224.5	66.7	27.3	651.0	69.6	40.7	212.7	65.9	26.7	609.0	71.6	43.3	213.1	61.9	26.8	625.4
2008	70.6	43.4	210.4	69.5	26.6	637.4	63.7	39.6	196.0	66.7	25.9	587.5	66.3	42.5	197.8	64.3	26.1	610.1
2009	62.4	39.7	212.6	75.3	28.1	634.6	57.3	36.5	195.6	69.8	27.0	580.5	59.0	39.3	201.6	68.7	27.4	610.5
2010	61.7	40.2	222.0	72.0	27.9	639.0	57.6	37.6	199.5	69.0	27.8	586.4	58.7	39.8	213.5	66.4	27.3	617.6
2011	62.9	38.5	216.3	70.7	27.1	630.7	57.3	35.5	196.1	68.7	27.0	577.8	59.0	37.9	206.9	64.9	26.6	607.9
2012	65.2	37.5	216.4	81.0	27.4	647.0	57.0	33.8	195.6	74.3	27.1	583.7	60.4	36.4	204.6	74.8	26.8	618.0
2013	59.3	36.1	203.2	75.0	27.9	618.9	54.5	33.4	189.4	71.6	27.6	572.0	55.7	36.0	193.5	68.9	27.4	596.7
2014	57.0	34.9	193.3	75.5	27.7	605.6	52.5	32.5	184.1	72.4	27.4	562.5	54.1	34.8	184.1	69.7	27.0	585.0
2015	54.4	35.4	182.4	74.9	27.7	596.0	50.5	32.7	175.5	71.3	27.4	553.8	51.6	34.8	174.2	69.1	27.1	574.2
2016	50.3	34.7	179.9	78.1	27.6	591.2	46.8	32.3	174.7	71.4	27.7	549.0	47.2	34.0	172.2	71.8	27.2	569.0
2017	50.4	34.8	175.4	78.2	25.8	583.6	46.6	32.6	175.4	73.0	26.7	549.9	47.1	33.9	169.0	71.9	25.4	562.2
2018	48.6	35.1	175.1	79.4	27.0	586.6	45.1	32.3	174.6	73.7	27.1	547.8	46.0	34.4	167.0	73.5	26.6	565.7
2019	46.4	34.1	168.8	79.4	27.5	577.5	43.7	32.1	169.9	74.8	27.3	544.6	44.5	33.6	162.3	72.8	27.0	557.3
2020	48.4	34.5	165.2	71.8	27.8	570.1	43.9	32.0	167.8	69.6	27.5	537.9	45.9	33.6	157.2	66.9	26.9	547.6
2021	48.2	34.0	149.0	77.5	25.5	553.3	43.8	31.7	158.5	72.7	26.3	525.9	47.6	33.9	143.5	72.4	23.9	538.9
2022	45.3	34.3	146.5	79.6	25.0	546.1	42.9	32.1	157.2	73.8	26.3	525.4	42.8	33.2	141.3	74.6	23.8	522.9

Table S1. Annual total anthropogenic CO emissions from 2003 to 2022, constrained with MOPITT column and profile data driven with the fixed and variable OH fields. The region definition is shown in Figure S1e.

	MOPITT Column + fixed OH (Tg/yr)							MOPITT Profile + fixed OH (Tg/yr)							MOPITT Column + variable OH (Tg/yr)						
Years	Boreal N. America	Boreal Asia	S. America	Africa	SE. Asia	Australia	Global	Boreal N. America	Boreal Asia	S. America	Africa	SE. Asia	Australia	Global	Boreal N. America	Boreal Asia	S. America	Africa	SE. Asia	Australia	Global
2003	20.6	70.6	42.7	158.6	13.0	16.6	365.6	17.2	79.3	42.1	146.6	14.0	15.5	355.6	18.1	69.2	39.5	152.9	13.3	16.2	351.2
2004	30.7	19.3	60.8	160.3	26.0	19.3	356.2	30.3	18.1	62.1	144.6	28.5	17.3	337.3	28.9	19.8	55.0	155.7	25.9	18.9	342.3
2005	21.7	24.6	63.5	178.3	18.1	8.7	357.8	18.9	22.2	67.1	164.7	19.4	7.8	338.8	20.6	22.1	57.3	171.4	17.8	8.3	338.9
2006	12.4	35.3	34.3	149.3	27.3	19.9	319.3	12.0	34.6	33.9	133.9	40.2	16.6	309.9	11.6	34.5	31.4	144.0	26.2	18.6	305.7
2007	10.7	27.7	68.6	166.6	15.2	16.7	361.7	10.3	24.2	76.3	148.1	12.8	14.6	333.2	10.1	26.6	64.3	159.8	14.7	16.2	346.0
2008	11.4	41.8	25.4	175.6	8.5	9.0	312.1	10.1	45.0	25.9	153.8	7.7	7.9	285.5	10.4	41.1	22.8	168.8	8.3	8.7	298.6
2009	13.5	23.8	13.2	151.9	44.4	16.8	309.7	11.6	22.9	14.3	128.4	46.9	14.9	278.3	13.5	23.1	11.6	148.0	43.4	16.3	301.0
2010	17.8	29.8	65.7	165.4	13.6	5.0	349.0	17.5	26.4	69.0	148.7	12.0	4.7	322.9	16.7	29.3	58.7	159.0	13.2	4.9	332.0
2011	11.8	35.3	18.3	171.3	14.5	29.0	312.5	12.7	30.8	18.8	148.5	16.0	24.6	279.7	11.1	33.5	16.6	164.3	14.1	28.2	298.6
2012	15.1	73.9	35.0	168.2	16.2	28.2	376.0	13.0	74.5	36.5	148.4	16.9	23.5	344.9	12.8	65.3	32.8	160.7	16.0	27.1	352.3
2013	22.7	39.6	14.8	170.4	15.4	11.3	310.9	24.1	35.4	16.7	147.8	15.9	9.6	282.0	21.0	35.3	13.2	164.6	14.8	11.1	295.6
2014	20.5	42.2	25.2	156.5	26.8	16.5	330.0	20.0	38.7	23.7	135.9	29.9	14.3	299.7	19.4	40.7	21.2	146.1	25.8	16.2	310.1
2015	25.3	40.7	37.1	169.4	34.6	13.0	362.1	27.1	42.5	36.8	149.8	46.0	11.2	353.0	23.5	39.7	33.7	164.0	34.4	12.6	348.7
2016	8.0	56.7	30.1	188.7	13.7	7.8	341.6	9.0	55.8	30.8	167.4	12.9	6.9	315.6	7.5	50.1	25.9	179.7	13.4	7.5	319.2
2017	22.8	36.0	40.6	174.8	6.6	16.9	337.7	22.8	33.9	38.3	156.0	6.6	14.3	308.4	20.9	32.1	34.3	166.1	6.4	16.1	313.7
2018	26.7	41.2	17.0	171.7	11.8	18.0	324.3	30.6	40.9	18.4	151.3	13.0	15.1	303.3	22.3	36.1	15.0	166.3	11.4	17.8	305.0
2019	20.5	58.5	38.0	170.7	26.1	27.0	379.9	24.8	55.6	35.0	148.1	29.9	34.6	364.4	17.9	51.0	33.8	164.3	25.6	26.5	356.9
2020	1.5	54.5	49.6	166.8	13.7	8.3	350.0	1.7	53.6	51.7	154.7	11.9	7.8	338.6	9.5	37.4	36.7	152.1	18.6	15.3	306.4
2021	79.1	129.1	31.8	177.9	9.9	7.1	477.9	91.9	172.0	31.7	158.7	9.9	6.6	515.6	52.2	102.6	26.7	154.5	17.0	14.7	401.4
2022	15.4	26.9	36.5	157.8	4.2	6.5	277.4	19.0	27.1	38.5	139.9	4.2	6.1	264.1	12.8	31.1	35.5	147.4	19.3	15.2	291.4

Table S2. Annual total biomass burning CO emissions from 2003 to 2022, constrained with MOPITT column and profile data driven with the fixed and variable OH fields. The region definition is shown in Figure S1f.

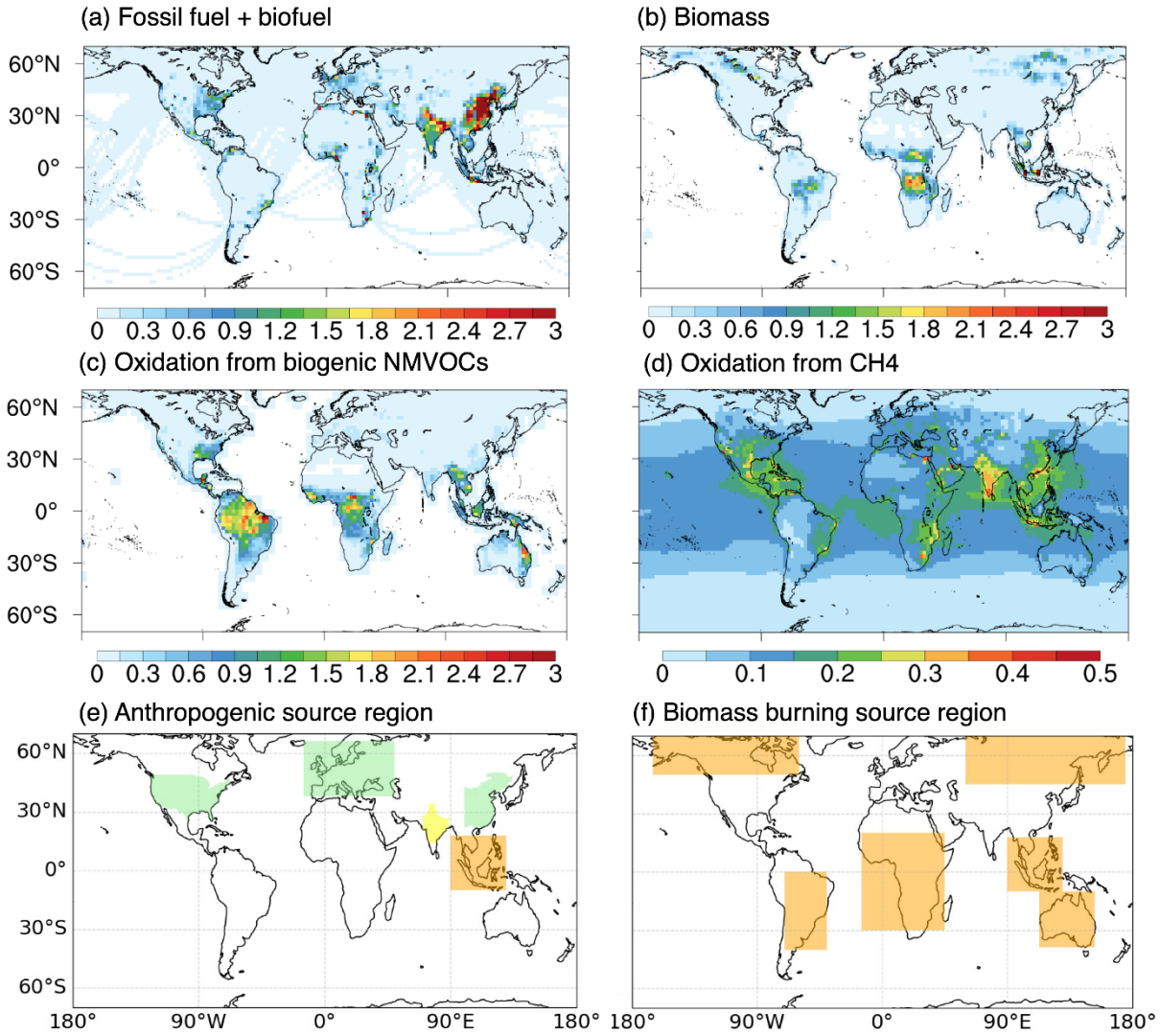

Fig. S1. (a-d) Mean a priori CO sources from 2003 to 2022 with unit 10^{12} molec/cm^2/sec; (e-f) Region definitions for (e) anthropogenic and (f) biomass burning sources. Since Eastern China, India, and Southeast Asia are geographically adjacent, different colors are used in Fig. S1e to distinguish these three regions.

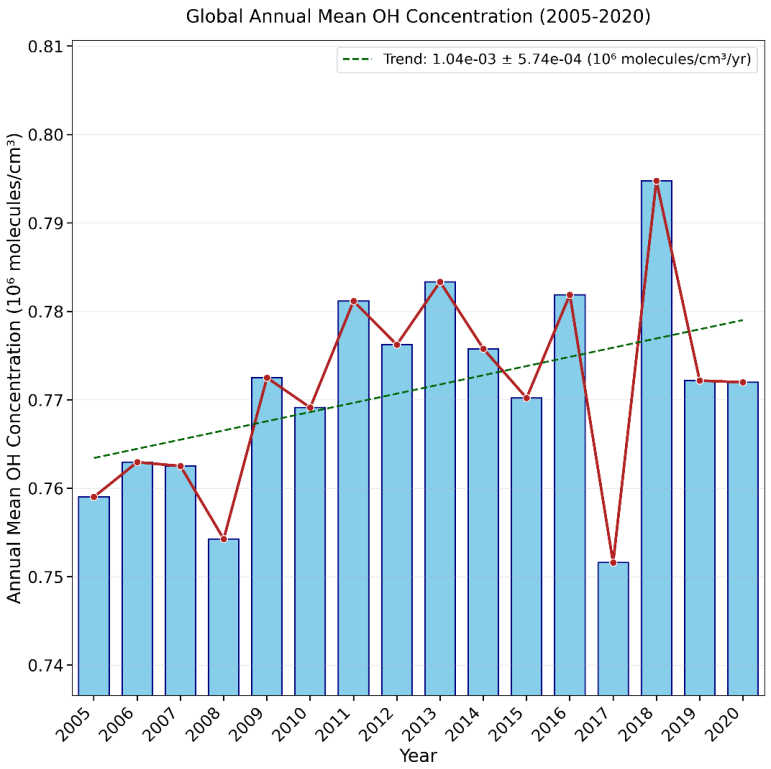

Fig. S2. Interannual variability of global mean tropospheric OH concentrations (2005-2020) from the TCR-2 tropospheric chemistry reanalysis.

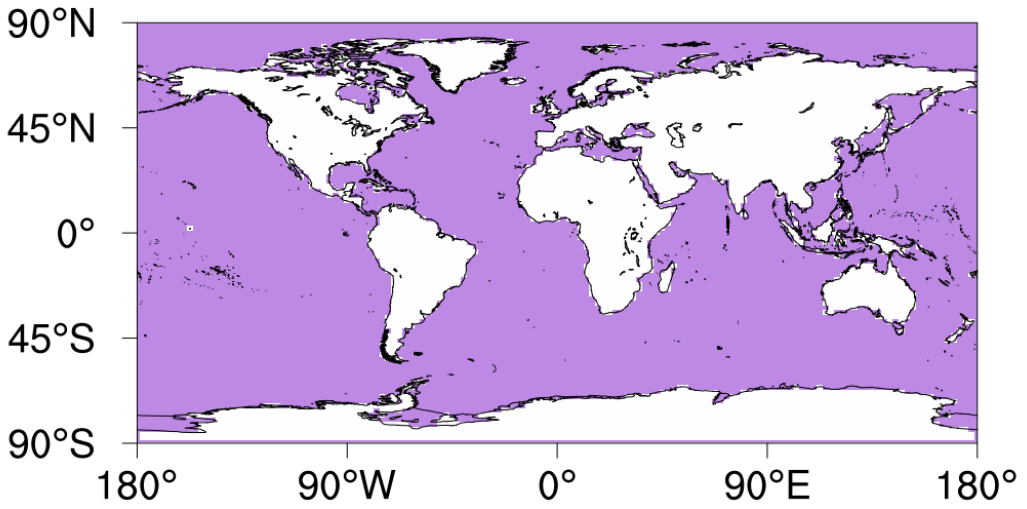

Fig. S3. Definition of the ocean boundary conditions. CO abundances over ocean (pink grids) were rewritten using the optimized hourly CO fields from Kalman Filter. The Kalman filter run is completely independent of the 4-DVAR inversions. There is no feedback of the 4-DVAR inversion results to the boundary conditions.

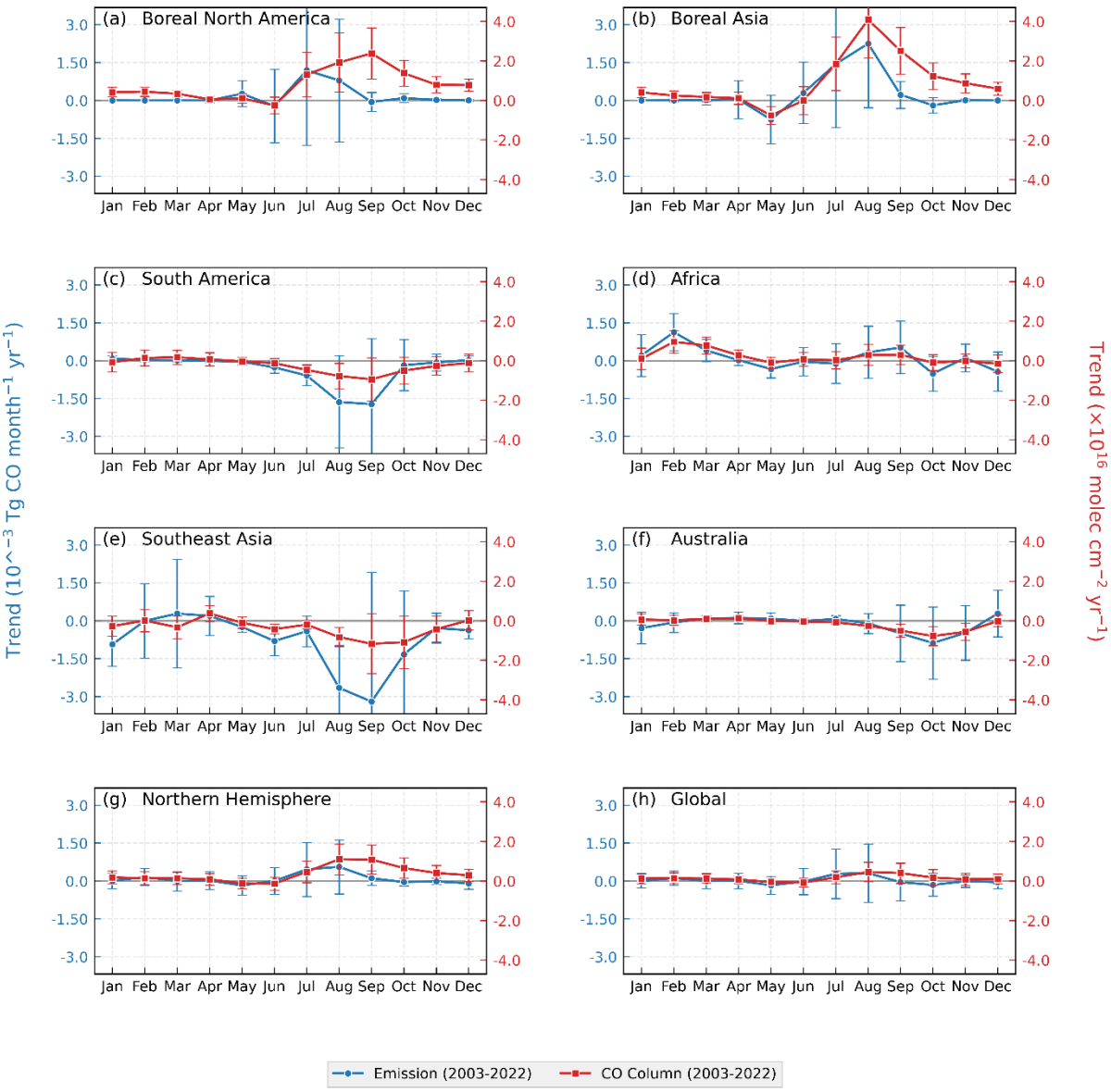

Fig. S4. Monthly trends in biomass burning CO emissions and in CO column concentrations attributable to biomass burning emission changes from 2003 to 2022, derived using the Column-FixOH method. Error bars indicate the standard deviation of the trends based on linear fitting.

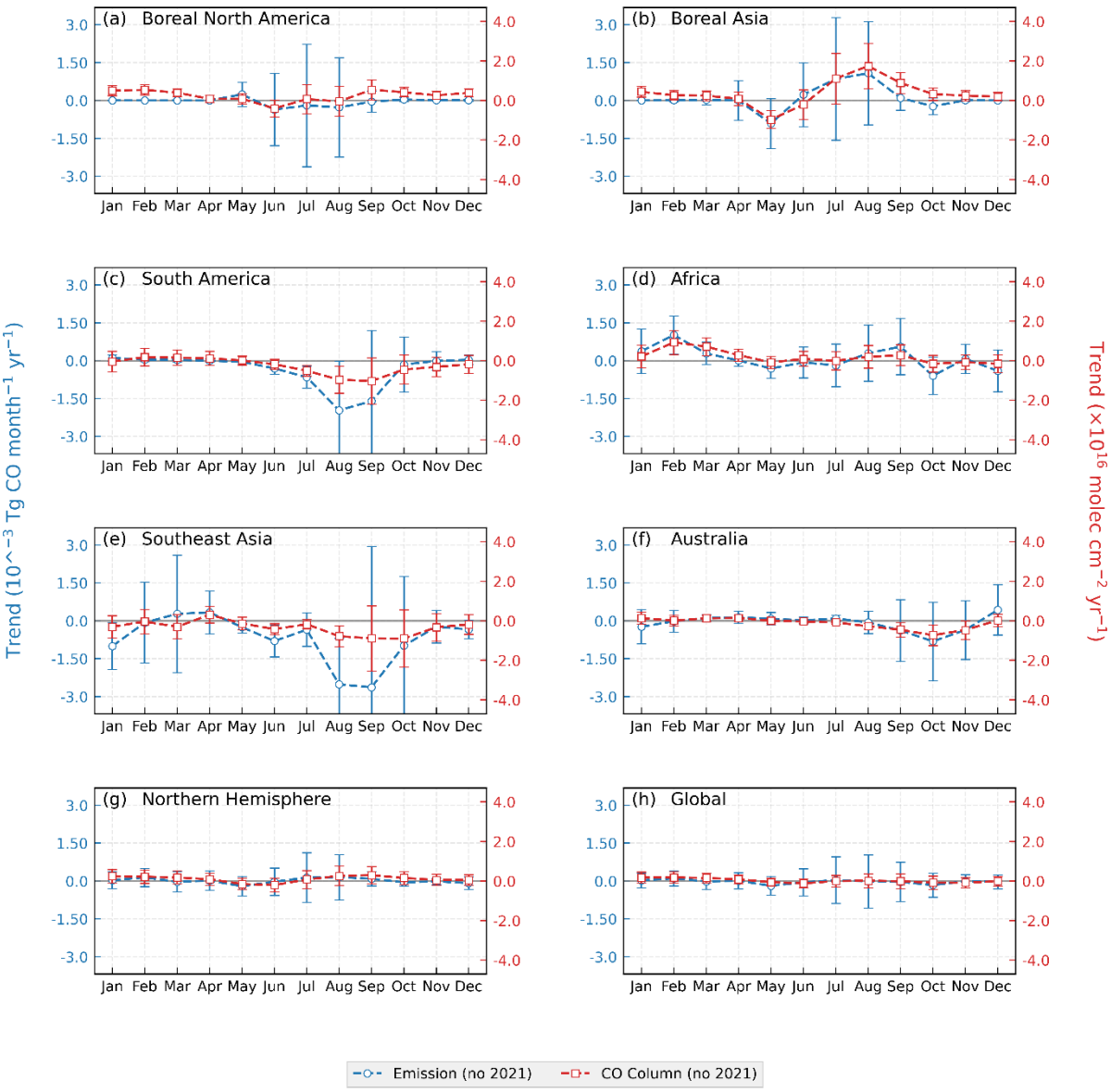

Fig. S5. Monthly trends in biomass burning CO emissions and in CO column concentrations attributable to biomass burning emission changes from 2003 to 2022, derived using the Column-FixOH method. Error bars indicate the standard deviation of the trends based on linear fitting. The year of 2021 was excluded from the trend calculation.